Computer-Aided Design 45 (2013) 195–203

Contents lists available at SciVerse ScienceDirect

Computer-Aided Design

journal homepage: www.elsevier.com/locate/cad

Compliance optimization of a continuum with bimodulus material under multiple load cases

Kun Cai [a,b,1], Zhaoliang Gao [c,*,1], Jiao Shi [a]

[a] College of Water Resources and Architectural Engineering, Northwest A&F University, Yangling 712100, China
[b] College of Engineering and Computer Science, The Australian National University, Canberra, ACT 2601, Australia
[c] Institute of Soil and Water Conservation, Northwest A&F University, Yangling, China

ARTICLE INFO

Article history:
Received 11 January 2012
Accepted 22 July 2012

Keywords:
Topology optimization
Bimodulus material
Multiple load cases
Material-replacement method

ABSTRACT

Topology optimization of a continuum with bimodulus material under multiple load cases (MLC) is investigated by using material replacement method. Using traditional methods to solve such a problem will encounter two difficulties for the sake of the stress-dependent behavior of bimodulus material. One is the nonlinear behavior of bimodulus material. The other is the definition of local material property under MLC. The present method can overcome the difficulties easily. It contains three major aspects. Firstly, the bimodulus material is replaced with two isotropic materials in optimization. Secondly, the local stiffness is modified according to the stress states because of material replacement. Meanwhile, which one of the isotropic materials to be adopted for each element in the next structural analysis in optimization is determined by the replacement criterion under MLC, i.e., comparing the local CSED (strain energy density (SED) caused by compression stresses) and the TSED (SED caused by tension stresses), the isotropic material which modulus equal to the compression modulus of bimodulus material is used as the material properties of the element if the CSED is greater than the TSED, or vice versa. Finally, the relative densities of elements as the design variables are updated using a gradient-based method. As the reanalysis with respect to material properties for obtaining the accurate deformation is merged into the global iterations of optimization, the efficiency of optimization is highly improved. Numerical examples are given to express the validity and high efficiency of the present method. Results also show that the difference between tension modulus and compression modulus influences the optimal topology of a structure with bimodulus material under MLC, obviously.

1. Introduction

The design optimization of a structure can be classified as the detailed designs (e.g., size and shape optimization) and the conceptual designs (e.g., topography and topological optimization (firstly envisioned by Maier [1])). In a size/shape optimization, only structural geometry is modified and the material layout stays unchanged. But, in topology optimization, which is utilized in the stage of conceptual design, the material layout changes in the design domain to obtain an optimal design for loadings. Around the world, the first popular software for solving large-scale continuum topology optimization is "SHAPE" [2,3]. In a practical engineering, the computational cost of topology optimization is usually much heavy. In the past 20 years, with the development of computer technology and computational methods [4–10], structural topology optimization in nowadays is becoming a powerful tool to find novel designs in various design fields [11,12], e.g., MEMS [13,14], laminated composites [15–18], acoustics [19], fluidics [20], and electromagnetism [21].

Such materials as concrete/cement, cast iron, membrane, fibers, are used widely in engineering. The tensile and compressive mechanical behaviors of the materials are different for micromechanisms or macrostructural buckling. However, their mechanical behavior usually behaves linearly. Generally, we call the materials as bimodulus materials. For a structure with bimodulus material, the mechanical property of the material is stress-dependent and structural reanalysis is necessary for finding the accurate deformation [22,23]. The curves of constitutive law of the materials are piecewise linear. Sometimes the constitutive curve is approximated by a continuous differentiable curve [24]. Especially, in topology optimization of a continuum with bimodulus material,

* Corresponding author. Tel.: +86 29 87012850, +86 13720779868.
E-mail address: coopcg@163.com (Z. Gao).
[1] Equal first authors.

0010-4485/$ – see front matter © 2012 Elsevier Ltd. All rights reserved.
doi:10.1016/j.cad.2012.07.009

such an approximate method is very popular. For example, [25] adopted proportional dual potential to give a continuous expression of material properties for bimodulus material. Chang et al. [26] approximated the piecewise linear curve with the first kind Chebyshev polynomial curve. Liu and Qiao [27] used a Heaviside function to approximate the relationship between stress and strain of bimodulus material.

In optimization of a structure with nonlinear material, the update both of material mechanical property and of the design variables should be carried out, separately. Meanwhile, the computer time is also influenced by the mesh scheme of the structure, e.g., a fine mesh gives accurate results and simultaneously increases computational cost. As simplicity, high efficiency and stability are the essentials of a method in application [28], people tried to find a method with such merits to solve bi-modulus stiffness designs. For instance, a material replacement method is worth considering. For example, [29,30] investigated the optimization of material-oriented structures by using different materials to resist the tension and compression forces. Alfieri et al. [31] proved the method and used the local maximum magnitude of the principal stress to determine local material property in design domain. Cai and Shi [32] presented a double reference interval method to solve such problems, and in that method the bimodulus material is replaced with an isotropic material and the porosity of the material changes according to the local principal strains. Bimodulus layout optimization was also studied by Srithongchai and Dewhurst [33]. Querin et al. [34] suggested orthotropic materials to replace the original bimodulus material in structure. Cai [35] once gave a modified SIMP method to solve the tension/compression-only stiffness design. In that approach, the tension/compression-only material is replaced with only one isotropic material. The modulus of the isotropic material is identical to the effective modulus of the tension/compression-only material. To consider the effects of tension/compression-only on local stiffness, the stiffness matrix of each element was modified. Numerical results demonstrated the validity of the idea of material replacement.

A structure under multiple load cases (or conditions) is very common in practical engineering. To solve the topology optimization of a structure under MLC, one of the major tasks is to give a reasonable objective function [36–39]. A weighted function on each load case is commonly used. But to our knowledge, no work published deals with bimodulus stiffness design under MLC. Because using traditional methods to solve bimodulus material layout optimization under MLC will encounter two difficulties for the sake of mechanical behavior of bimodulus. One is the stress-dependent of material, which means the material principal directions are aligned with those of principal stresses and structural reanalysis is necessary. The other is the definition of local material property under MLC, which is also caused by stress-dependent behavior.

In this research, we attempt to give a method for optimal stiffness design of structures with the bi-modulus material under MLC. This paper is organized as follows: Section 2 introduces the concept of bimodulus material, Section 3 shows the techniques of the proposed method, Section 4 gives several numerical examples to demonstrate the effectiveness of the present approach. Finally, some conclusions are drawn in Section 5.

2. Bimodulus material

Fig. 1 gives the stress–strain curve of a material. For linear material, the tangent value of the angle α gives the tension modulus of material, and the tangent value of β is the compression modulus. As $\alpha = \beta$, we call the material as isotropic material. But for many materials in engineering, such as cast iron, rubber, concrete, the difference between α and β is obvious. So, the

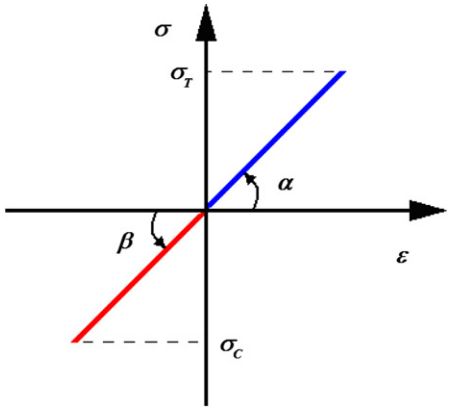

Fig. 1. The stress–strain ($\sigma-\varepsilon$) curve.

stress–strain curve is piecewise linear, and the material is commonly called a bimodulus material. As the material properties are stress-dependent, in structural analysis, the material has to be considered as nonlinear and iterative analysis is inevitable [24,26,27]. To simplify the structural analysis, the character of the curve, i.e., piecewise linear, should be considered [31,34,35].

For a bimodulus material, the tension modulus E_T and the compression modulus E_C can be expressed as

$$\begin{aligned} E_T &= \tan\alpha \\ E_C &= \tan\beta. \end{aligned} \tag{1}$$

The ratio between E_T and E_C is signed as

$$R_{\mathrm{TCE}} = \frac{E_T}{E_C}. \tag{2}$$

In Fig. 1, σ_T and σ_C are the allowable stresses of material under tension and compression respectively. They can also be different for a practical material. Clearly, the difference between σ_T and σ_C has no relation with the difference between E_T and E_C. In this work, the effects of the difference between σ_T and σ_C on optimal material distribution in structure [40,41] are not under consideration.

3. Methodology

A finite element method is adopted to solve the mechanical response of the structure under multiple load cases, and only a small deformation is under consideration in this work. To avoid the structural reanalysis for material nonlinearity, the original bimodulus material is replaced with two isotropic materials with moduli equal to the tension and compression moduli of the bimodulus material, respectively. The new techniques on solving the topology optimization of a continuum with bimodulus material under MLC are given below, and five steps are contained. Firstly, the optimization model is given in Section 3.1. Secondly, the relationship between the relative density and the modulus of porous material is introduced in Section 3.2 and the power-law is adopted. Thirdly, the selection of modulus of an element is introduced in Section 3.3. Fourthly, to consider the difference between the mechanical behaviors of structure with new materials or with original bimodulus material, the modification of local stiffness is introduced in Section 3.4. Fifthly, the update of design variables is discussed in Section 3.5. Finally, the flow chart of the present algorithm is shown in Section 3.6.

3.1. Optimization model

Under multiple load cases, the volume constrained optimization of a structure with minimum of the structural mean

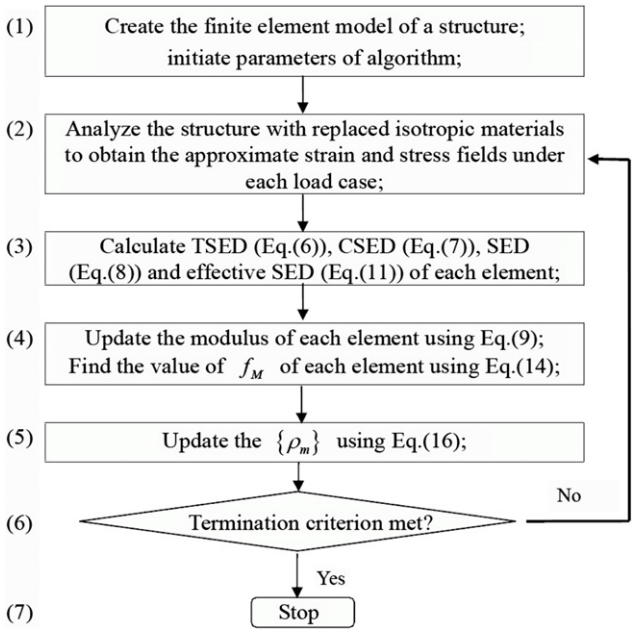

Fig. 2. Flow chart of the present algorithm.

compliance can be expressed as

$$\begin{aligned} &\text{Find}: \quad \{\rho_m | m \in \Omega\} \\ &\min_{\{\rho_m\}}: \quad c = \sum_i^I \boldsymbol{U}_i^T \overline{\boldsymbol{K}}_i \boldsymbol{U}_i = \sum_i^I \sum_{m=1}^M \left(\boldsymbol{u}_m^T \overline{\boldsymbol{k}}_m \boldsymbol{u}_m\right)_i \\ &\text{subject to}: \quad \frac{1}{V_0} \sum_i^I \sum_{m=1}^M (\rho_m v_m)_i = r_v \\ &\qquad \boldsymbol{K}_i \boldsymbol{U}_i = \boldsymbol{P}_i, \quad i = 1, 2, \ldots, I \\ &\qquad 0 < \rho_{\min} \le \rho_m \le 1.0, \quad m \in \Omega \end{aligned} \tag{3}$$

where the objective function c, is the sum of the structural mean compliances of the load cases. I is the number of load cases the structure is subjected to. M is the total number of elements. $\{\rho_m\}$ is the set of relative densities of elements. $\boldsymbol{U}_i$ and $\boldsymbol{P}_i$ are the global nodal displacement and force vectors in the i-th load case, respectively. $\boldsymbol{k}_m$ is the stiffness matrix of the m-th element with an isotropic material. $\overline{\boldsymbol{k}}_m$ is the modified matrix of $\boldsymbol{k}_m$. $\boldsymbol{K}_i$ is the global stiffness matrix of the structure assembled with $\{\boldsymbol{k}_m\}_i$. $\overline{\boldsymbol{K}}_i$ is assembled with $\{\overline{\boldsymbol{k}}_m\}_i$. $\boldsymbol{u}_m$ is the nodal displacement vector of the m-th element. To avoid the singularity of $\boldsymbol{K}_i$ with fixed finite element mesh, $\rho_{\min} = 0.001$ is used in the present work. v_m is the volume of the m-th element. V_0 is the total volume of solid design domain. Positive scalar r_v is the critical volume ratio of the final structure.

3.2. Elastic modulus of a porous material

Topology optimization of a structure only with solid material and void, is commonly considered as an integer programming problem with discrete design variables of 1 and 0. The computational cost of the problem is extremely high when the number of elements is huge. The gradient based methods cannot be applied to solve the problem directly. Therefore, generally, the same optimization problem is relaxed to be with continuous design variables and is solved by gradient-based methods. In the present work, the material in an element is considered as a porous material. And the relative density of material can change in the interval $[\rho_{\min}\ 1]$ continuously. Thus, the local mechanical properties become differentiable functions associated with the relative density.

A power-law relationship is used to penalize intermediate densities [42] to obtain a result close to the original binary design. For an element, e.g., the m-th element, the relationship between the stiffness tensor and the relative density can be expressed as

$$D_{m,ijkl} = \rho_m^p D_{0,ijkl} \tag{4}$$

$$D_{0,ijkl} = \lambda \delta_{ij} \delta_{kl} + \mu \left(\delta_{ik} \delta_{jl} + \delta_{il} \delta_{jk}\right) \tag{5}$$

where the relative density $\rho_m \in \left[\rho_{\min} \quad 1.0\right]$, the power p is the penalization factor. In the present work, $p = 3$ is used. $D_{m,ijkl}$ is the stiffness tensor of the porous material and $D_{0,ijkl}$ is the stiffness tensor of the solid material with Lame constants of λ and μ. δ_{ij} is the Kronecker delta.

3.3. Selection of local isotropic material

As the original bimodulus material is replaced with two isotropic materials and only one of them can be used as the material of each element for structural analysis. It is known, under a single load case, the mechanical behavior of bimodulus material is determined by the local stress state. Therefore, the isotropic material to be used as the local material is completely determined by the local stress state. For example, if all of the principal stresses of an element are negative the element is under pure compression, and the new isotropic material with modulus equal to the compression modulus of bimodulus material can accurately express the local material property. Pure tension will also tell us the isotropic material whose modulus is equal to the tension modulus of the biomodulus material is the correct selection of the local material property. Under complex stress state, i.e., the 1st principal stress is positive while the 3rd is negative, the bimodulus material shows orthotropic (transversally isotropic in detail) and any one of the isotropic materials cannot be used to express the accurate local material property. But in the material-replacement method, one of the two isotropic materials must be used to approximately express the local material properties. And the difference of local stiffness caused by the replacement will be modified and is discussed in the next section. Now, which one of the isotropic materials should be selected as the material of an element under a complex stress state? This situation becomes more serious under MLC. Here we define the tension strain energy density (TSED) as the strain energy density caused by positive principal stresses and the compression strain energy density (CSED) as the strain energy density caused by negative principal stresses. For the m-th element under MLC, the TSED and CSED can be obtained by the following equations.

$$\text{TSED}_m = \frac{1}{2N_G} \sum_{i=1}^{I} \sum_{\text{Gaus}=1}^{N_G} \sum_{j=1}^{3} \frac{1}{2} \left(\sigma_{j,\text{Gaus},i} + \left|\sigma_{j,\text{Gaus},i}\right|\right) \cdot \varepsilon_{j,\text{Gaus},i} \tag{6}$$

$$\text{CSED}_m = \frac{1}{2N_G} \sum_{i=1}^{I} \sum_{\text{Gaus}=1}^{N_G} \sum_{j=1}^{3} \frac{1}{2} \left(\sigma_{j,\text{Gaus},i} - \left|\sigma_{j,\text{Gaus},i}\right|\right) \cdot \varepsilon_{j,\text{Gaus},i} \tag{7}$$

where N_G is the number of Gaussian integrating points of an element. $\sigma_{j,\text{Gaus},i}$ and $\varepsilon_{j,\text{Gaus},i}$ are the principal stress and strain, respectively.

The total SED of the element is

$$\text{SED}_m = \text{TSED}_m + \text{CSED}_m. \tag{8}$$

The elastic modulus of local material under MLC is determined by the following equation.

$$E_m = \begin{cases} E_T, & \text{if (TSED} > \text{CSED)} \\ E_C, & \text{if (TSED} < \text{CSED)} \\ \max(E_T, E_C), & \text{others.} \end{cases} \tag{9}$$

The method is different from the method for selection of material given by Alfieri et al. [31] in which the material properties are determined by local principle stresses.

3.4. Calculation of $\overline{\boldsymbol{k}}_m$ and Modification of local stiffness

In simulation, the stiffness matrix of the m-th element before modification reads

$$\boldsymbol{k}_m = \int_{v_m} \boldsymbol{B}_m^T \boldsymbol{D}_m \boldsymbol{B}_m \mathrm{d}v \tag{10}$$

where $\boldsymbol{B}_m$ is the geometric matrix to relate the strain and the nodal displacement of an element. $\boldsymbol{D}_m$ is the elastic matrix of an element with isotropic material.

As the elastic matrix of the element with original material is different from the "current" matrix, i.e., $\boldsymbol{D}_m$, the "current" element stiffness matrix $\boldsymbol{k}_m$ must be different from the accurate matrix, which further influences the local mechanical behavior. To reduce the difference after material replacement, the matrix $\boldsymbol{k}_m$ should be modified.

The criterion of modification for local stiffness is given according to the local strain energy under the "current" stress state. Briefly, the effective SED of the element under the "current" stress state may be different from the "current" SED (Eq. (8)). Thus, the effective strain energy density (SED) of the m-the element should be expressed as

$$\mathrm{SED}_m^{\mathrm{effective}} = \frac{1}{2N_G} \sum_{i=1}^{I} \sum_{\mathrm{Gaus}=1}^{N_G} \sum_{j=1}^{3} \left(\mathrm{sign}(\sigma_{j,\mathrm{Gaus},i}) \cdot \sigma_{j,\mathrm{Gaus},i} \cdot \varepsilon_{j,\mathrm{Gaus},i}\right). \tag{11}$$

Two cases are discussed in determining the value of sign(·) in Eq. (11).

(a) If the "current" modulus of material in an element is E_T, Eq. (12) is used to obtain the value of sign(·).

$$\mathrm{sign}\left(\sigma_j\right) = \begin{cases} 1 & \text{if } \sigma_j \geq 0 \\ R_{\mathrm{TCE}} & \text{if } \sigma_j < 0. \end{cases} \tag{12}$$

(b) If the "current" modulus of material in an element is E_C, Eq. (13) is used to obtain the value of sign(·).

$$\mathrm{sign}\left(\sigma_j\right) = \begin{cases} 1 & \text{if } \sigma_j \leq 0 \\ R_{\mathrm{TCE}}^{-1} & \text{if } \sigma_j > 0. \end{cases} \tag{13}$$

Particularly, $R_{\mathrm{TCE}} = 1$ means the material is isotropic, and the effective SED of an element is absolutely equal to either the real SED or the "current" SED even under a complex stress state. When $R_{\mathrm{TCE}} \neq 1$, the effective SED and the current SED are not identical to each other. And the modification factor for local stiffness matrix is expressed as following equation.

$$f_M = \max\left(10^{-6}, \frac{\mathrm{SED}_m^{\mathrm{effective}}}{\max\left(10^{-30}, \mathrm{SED}_m\right)}\right). \tag{14}$$

Using Eqs. (4) and (10), the modified stiffness matrix $\overline{\boldsymbol{k}}_m$ can be expressed as

$$\overline{\boldsymbol{k}}_m = f_M \cdot \boldsymbol{k}_m = \left(f_M^{1/p} \cdot \rho_m\right)^p \int_{v_m} \boldsymbol{B}_m^T \cdot \boldsymbol{D}_0 \cdot \boldsymbol{B}_m \mathrm{d}v. \tag{15}$$

3.5. Update of design variables

The optimization problem in Eq. (5) is solved by the optimality criteria (OC) method [43,44]. For the m-th element at the k-th step, the update of its relative density is determined by the following equation.

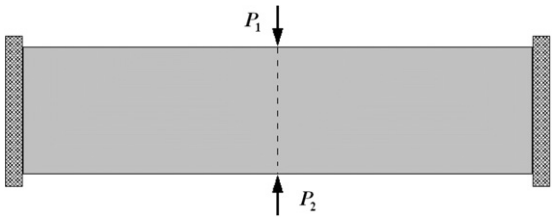

Fig. 3. Initial design of structure.

$$\rho_m^{(k+1)} = \begin{cases} \max\left\{\rho_{\min}, \rho_m^{(k)} - \Delta\right\} & \text{if } \rho_m^{(k)} L_m^q \leq \max\left\{\rho_{\min}, \rho_m^{(k)} - \Delta\right\} \\ \rho_m^{(k)} L_m^q & \text{others} \\ \min\left\{1.0, \rho_m^{(k)} + \Delta\right\} & \text{if } \rho_m^{(k)} L_m^q \geq \min\left\{1.0, \rho_m^{(k)} + \Delta\right\} \end{cases} \tag{16}$$

where Δ, i.e., the maximum incremental of relative density is set to be 0.1 in this work. Numerical damping coefficient $q = 0.5$, Using the optimality condition, one can obtain L_m according to the following equation.

$$L_m = \left| \frac{\partial c}{\partial \rho_m} \Big/ \left(\lambda \frac{\partial V_m}{\partial \rho_m}\right) \right|^{(k)} \tag{17}$$

$$\frac{\partial c}{\partial \rho_m} = p \rho_m^{-1} \sum_i^I \left(\boldsymbol{u}_m^T \overline{\boldsymbol{k}}_m \boldsymbol{u}_m\right)_i \tag{18}$$

where the positive scalar λ is the Lagrangian multiplier, which can be found by using the bi-sectioning algorithm. To avoid the checkerboards in optimization, the objective sensitivities, $\left\{\frac{\partial c}{\partial \rho_m}\right\}$, are modified by a filter technique [9,44,45].

3.6. Flow chart of algorithm

The termination condition in step 6 in Fig. 2 is given below.

$$\left|\frac{c_k - c_j}{c_k}\right| \leq \eta, \quad 1 < j = k-n, k-n+1, \ldots, k-1 \tag{19}$$

where the tolerance $\eta = 0.001$, integer n is set to be 5 in this work.

4. Results and discussions

Structural analysis in the following examples are performed by using commercial software ANSYS (version 12.0) [46]. A fixed finite element mesh is adopted in each example to describe the entire design domain in optimization. The same PC (Intel Pentium Dual-Core processor, CPU 2.66 GHz, 2 G Memory) with the same setting of computation is used in solving the following examples.

4.1. Example 1—isotropic vs bimodulus

Fig. 3 shows a deep beam with size of 4 m × 1 m and thickness of 0.02 m. Two vertical sides are fixed. The structure is discretized with 3600 plane stress elements. The tension modulus of the original bimodulus material is $E_t = 100$ GPa and the Poisson's ratio is 0.2.

Topology optimization of the structure under two load cases is considered. For the first load case, a concentrated force of P_1 is applied on the center of the top vertically. For the second load case, a concentrated force of P_2 is applied on the center of the bottom, vertically. The objective of optimization is to minimize the structural compliance with limited amount of material, e.g., the

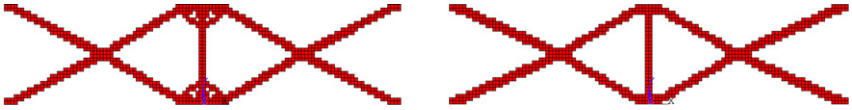

(a) With isotropic material (57 iterations). (b) With bimodulus material (60 iterations).

Fig. 4. The optimal topology of structure under two load cases symmetrically ($P_1 = P_2$).

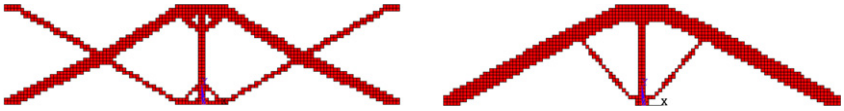

(a) With isotropic material (53 iterations). (b) With bimodulus material (32 iterations).

Fig. 5. The optimal topologies of structure under MLC ($P_1 = 1.4P_2$).

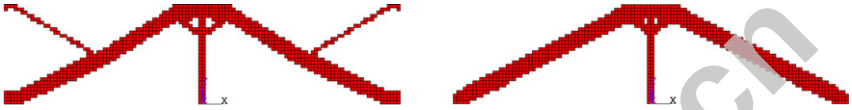

(a) With isotropic material (54 iterations). (b) With bimodulus material (44 iterations).

Fig. 6. The optimal topologies of structure under MLC ($P_1 = 2P_2$).

volume ratio of final structure, r_v in Eq. (3), is 20%. To show the effects of bimodulus on the final topology, the following six cases are considered.

(a) $P_1 = P_2 = 1000$ N and the material in structure shows isotropy, i.e., $R_{TCE} = 1/1$;
(b) $P_1 = P_2 = 1000$ N and $R_{TCE} = 1/2$;
(c) $P_1 = 1.4P_2 = 1400$ N and $R_{TCE} = 1/1$;
(d) $P_1 = 1.4P_2 = 1400$ N and $R_{TCE} = 1/2$;
(e) $P_1 = 2P_2 = 2000$ N and $R_{TCE} = 1/1$;
(f) $P_1 = 2P_2 = 2000$ N and $R_{TCE} = 1/2$.

• Results of cases (a) and (b)

The frame shown in Fig. 4(a) is the optimal isotropic material distribution for the structure (Fig. 3) under two load cases, and the structure shown in Fig. 4(b) is the structure with bimodulus material under the same loading conditions. Although both of the final structures have two symmetric planes, the topologies are different near the centers of top and bottom boundaries. The difference implies the stiffness design of a structure with bimodulus material cannot be replaced with traditional design (with isotropic material) even if the loading cases are symmetric.

• Results of cases (c) and (d)

Fig. 5 gives the optimal topologies of structure under two load cases with $P_1 = 1.4P_2$. Fig. 5(a) shows the traditional design (structure with isotropic material). For the sake of $P_1 > P_2$, the final structure has only one symmetric plane, and the amount of material under compression is greater than that under tension in the first load case.

Fig. 5(b) displays the optimal material distribution of the structure with bimodulus material under the same load cases. The topology is different from the traditional design (Fig. 5(a)), obviously. Under the first load case, the amount of material under compression in this figure (Fig. 5(b)) is greater than that of structure in Fig. 5(a). Therefore, bimodulus stiffness design, i.e., the stiffness design of a structure with bimodulus material, might be far different from the traditional design.

• Results of cases (e) and (f)

Fig. 6 gives the optimal material distributions for a structure with different materials under the same load cases ($P_1 = 2P_2$). The two topologies are different.

From above, one can find the topologies for all of the six cases are different from each other. So, the bimodulus stiffness design is different from the stiffness design with isotropic material. Simultaneously, in each of the above comparisons the iterations for the update of bimodulus material are not identical to that for the update of isotropic material. But the difference between them is not of significance.

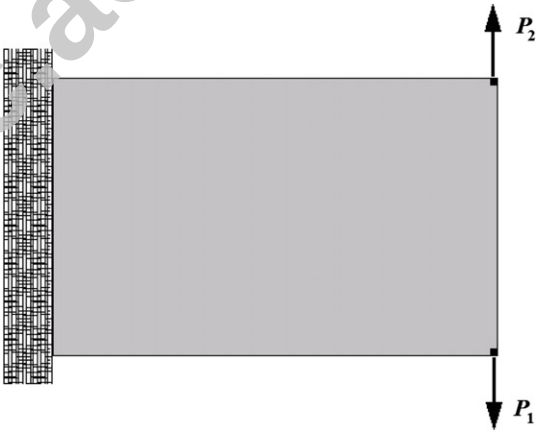

Fig. 7. Initial design of a cantilever beam under two load cases.

4.2. Example 2—effects of R_{TCE}

Fig. 7 shows a 0.8 m × 0.5 m cantilever beam with thickness of 0.02 m. The structure with left side fixed is under two load cases, e.g., $P_1 = 1000$ N on the lower right corner for case 1 and $P_2 = 1000$ N on the upper right corner for case 2. The structure is discretized with 2560 plane stress elements. The tension modulus of the bimodulus material is $E_t = 100$ GPa and the Poisson's ratio is 0.2. The objective is to minimize the structural compliance while the final structural volume ratio, r_v, is 30%.

Three cases on considering the differences between the tension and compression moduli are investigated to show the validity of the method, i.e.,

(a) $R_{TCE} = 4/5$ v.s. $R_{TCE} = 5/4$;
(b) $R_{TCE} = 1/2$ v.s. $R_{TCE} = 2/1$;
(c) $R_{TCE} = 1/8$ v.s. $R_{TCE} = 8/1$.

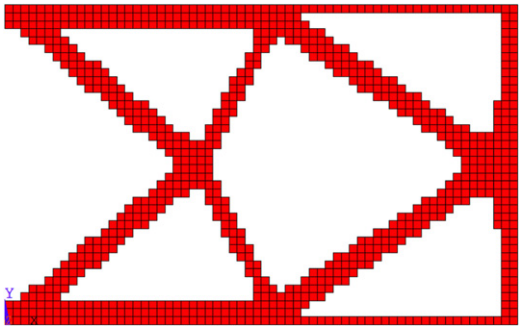

Fig. 8. Optimal topology of structure with isotropic material under MLC.

Fig. 8 gives the optimal topology of structure with isotropic material under multiple load cases. Here this result is called a traditional design, and is used for the comparison with the optimal design of structure with different bimodulus materials under the same loading cases (see Figs. 11–13).

Fig. 9 gives the optimal topologies of the cantilever beam under different single load cases. Circulating any one of the two topologies around the x-axis, one can find the two topologies are the same. The reason is that the two points where P_1 and P_2 are applied distribute symmetrically. And it also leads to the same results as the structure is filled with a bimodulus material. Therefore, Fig. 10 only gives the optimal material distributions of the structure with bimodulus under the first loading case. It also shows the difference of the topologies of structure for different values of R_{TCE}.

• Results of case (a)

Fig. 11(a) shows the optimal topology of structure with a bimodulus material of $R_{TCE} = 4/5$. The topology is identical to the traditional design (see Fig. 8) except the difference in local shapes in two frames. $R_{TCE} = 4/5$ implies that the compression modulus is 1.25 times the tension modulus. Meanwhile, the area near the concentrated forces must be under tension. The material layout in the rest area of the structure is easily under compression.

Fig. 11(b) gives the optimal structure with the bimodulus material of $R_{TCE} = 5/4$. It means the tension modulus of the material is 1.25 times the compression modulus. This topology is obviously different from the traditional design (Fig. 8), and is also different from that in Fig. 13(a).

It also can be concluded that the topologies in Fig. 11 are different from those in Fig. 10(a) and (b). For cases (b) and (c), differences exist, as well.

• Results of case (b)

Fig. 12(a) displays the optimal material distribution in a structure with the bimodulus material of $R_{TCE} = 1/2$, which is different from the traditional design, as well. The material adjacent to the right vertical side layouts is complicated.

The frame shown in Fig. 12(b) is the optimal structure with the bimodulus material of $R_{TCE} = 2/1$. The structure is also different from those in Figs. 8 and 13. The size of the X-shaped internal component is very small. So, the loads are mainly transferred to the fixed end (left vertical side) by the two strong inner arms.

• Results of case (c)

Fig. 13(a) and (b) give the final material distributions for the last two cases in which the two moduli of bimodulus material are greatly different. The material distributes to be easily under compression in Fig. 13(a), or to be easily under tension in Fig. 13(b).

4.3. Example 3—efficiency

In Fig. 14 the rectangle structure with sizes of 4.0 m × 1.0 m × 0.02 m is under three load cases. For the first case, the concentrated force of $P_1 = 1000$ N is applied on the point M_1. For the second case, the total 1000 N is separated into two parts ($P_2 = 500$ N) and applied on the points M_{21} and M_{22}, separately. For the third case, the total 1000 N is separated into two parts ($P_3 = 500$ N) and applied on the points M_{31} and M_{32}, separately. The tension modulus of the material is 10 GPa and Poisson's ratio is 0.2. The element size is 0.025 m. In the final structure, the volume ratio, r_v, is 35%.

To show the efficiency of the present method, two cases are discussed, i.e.,

(a) The material is isotropic, i.e., $R_{TCE} = 1$;
(b) The material is bimodulus, e.g., $R_{TCE} = 1/5$.

Fig. 15 shows the topologies of the structure subjected to a single load case for different conditions. Under the same loading case, the optimal topologies are different as the material in structure shows different mechanical behavior. Clearly, the topologies are different from those in Fig. 16. As compression modulus is much greater than tension modulus ($R_{TCE} = 1/5$), the material distribution in Fig. 16(b) is also different from that in Fig. 16(a). Comparing the topologies in Figs. 15 and 16, one can find the the first load case has the greatest effect on the final material distribution.

The result shown in Fig. 16(a) is obtained by using CPU time of 3935 s after 49 iterations (Fig. 17). The final structure in Fig. 16(b) is obtained by using a CPU time of 5275 s after 55 iterations (Fig. 17). It means the CPU time for the second case is 34% higher than that of the first case. The difference between the CPU times of each step for two cases is about 11.9%. The iterations of the second case is greater than that of the first case is merely coincidental.

The value of objective function, i.e., structural compliance reaches 0.69 N m for the first case, in which the material in the structure is isotropic. The objective function finally approaches 0.316 N m as the material in the structure shows bimodulus behavior. It is less than that of the first case. The reason is that the tension moduli are the same in two cases. However, the compression modulus is greater than tension modulus in the second case.

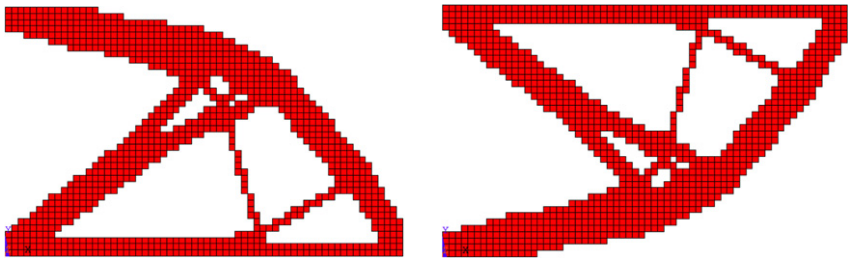

(a) Only P_1 acts. (b) Only P_2 acts.

Fig. 9. Optimal layouts of isotropic material under single load case.

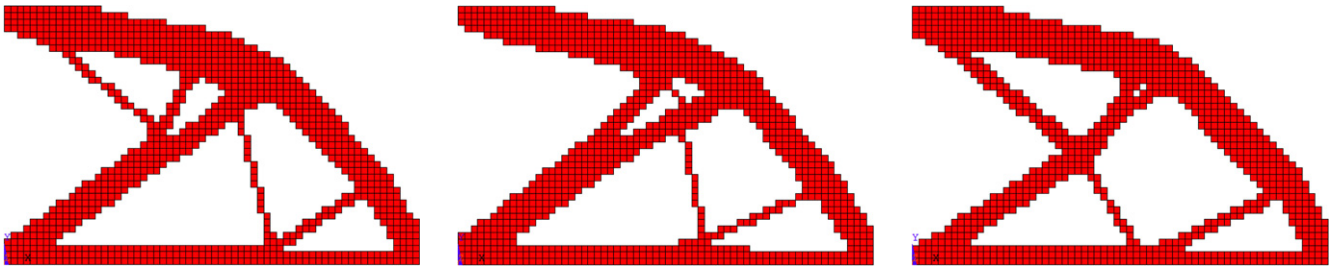

(a) $R_{TCE} = 4/5$. (b) $R_{TCE} = 5/4$. (c) $R_{TCE} = 1/2$.

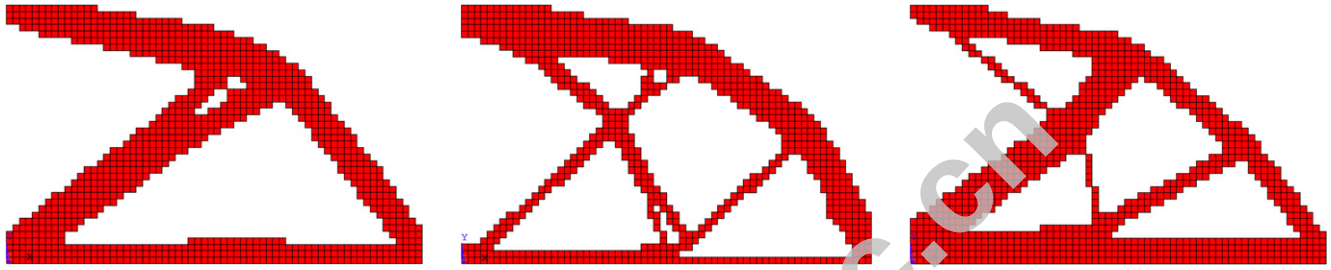

(d) $R_{TCE} = 2/1$. (e) $R_{TCE} = 1/8$. (f) $R_{TCE} = 8/1$.

Fig. 10. Optimal layouts of bimodulus material in structure only under P_1.

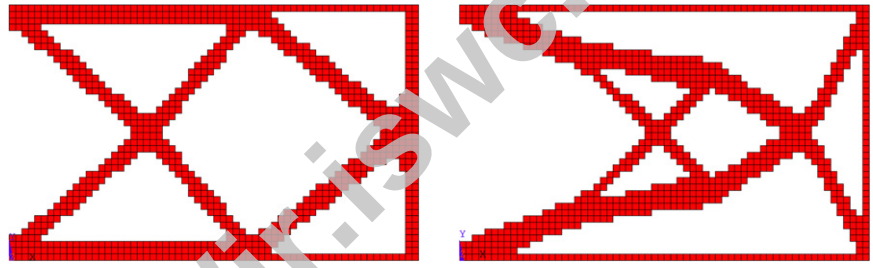

(a) $R_{TCE} = 4/5$. (b) $R_{TCE} = 5/4$.

Fig. 11. The optimal topologies of structure with different bimodulus materials (Case (a)).

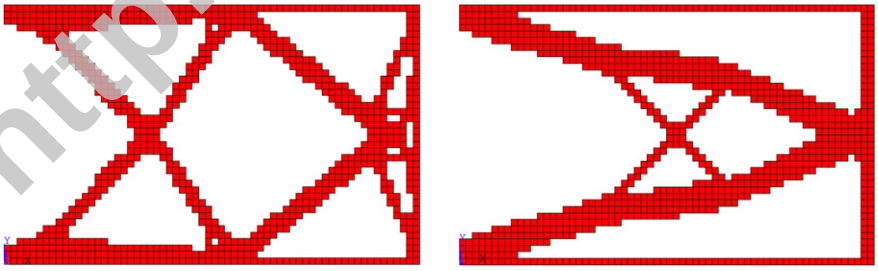

(a) $R_{TCE} = 1/2$. (b) $R_{TCE} = 2/1$.

Fig. 12. The optimal topologies of structure with different bimodulus materials (Case (b)).

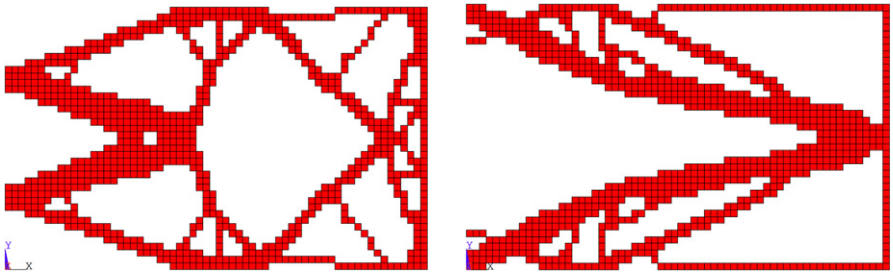

(a) $R_{TCE} = 1/8$. (b) $R_{TCE} = 8/1$.

Fig. 13. The optimal topologies of structure with different bimodulus materials (Case (c)).

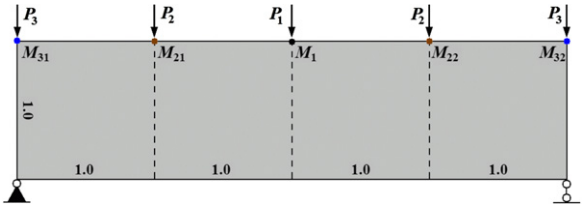

Fig. 14. Initial design of structure.

5. Conclusions

The material-replacement method is applied to investigate the optimal topology of a continuum with bimodulus material under multiple load cases. From numerical results, some conclusions are obtained as follows

(1) The final topology of a structure with bimodulus material under multiple load cases is different from that of the same structure with isotropic material under the same loading conditions. Especially, if the loads applied on structure are not of symmetry, the difference of topologies is much obvious and should be paid attention to in practical engineering.
(2) The value of R_{TCE} (or the ratio between E_t and E_c) influences the final topology, greatly, e.g., the amount of materials under compression tends to be greater when R_{TCE} is less than 1.0, and vice versa.
(3) Under the same MLC, the computational cost of topology optimization of a continuum with bimodulus is slightly greater than that of the structure with isotropic material per iteration because different update schemes for design variables. However, the iteration number for bimodulus update is not definitely greater than that for isotropic materials update.

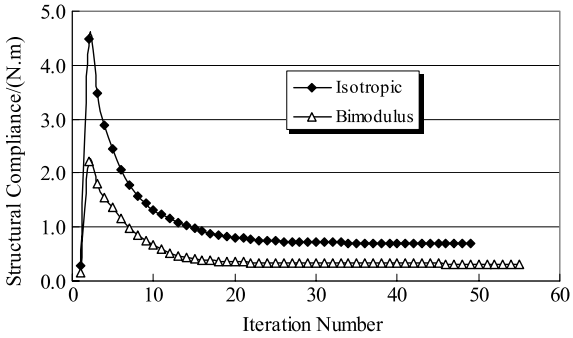

Fig. 17. Iteration histories of mean compliances of structure with different materials.

(4) As bimodulus material being stress-dependent, under MLC the local stress state is not an accurate concept which confuses the update of design variables in traditional methods. Using the present method, the local bimodulus material is replaced with one of two isotropic materials and the effective strain energy density becomes the role for modulus selection. Numerical results show its simplicity and effectiveness which is easy operating in practical engineering.

Acknowledgments

Support for this research was provided by the National Natural Science Foundation of China (Grant No. 50908190, 51179164), the Fundamental Research Foundation of Northwest A&F University (Grant No. QN2011125) and Open Research Foundation (PF2011-21) of State Key Lab of Information Engineering, Mapping and Remote Sensing, Wuhan University, China. Thanks to the anonymous reviewers for their meaningful suggestions.

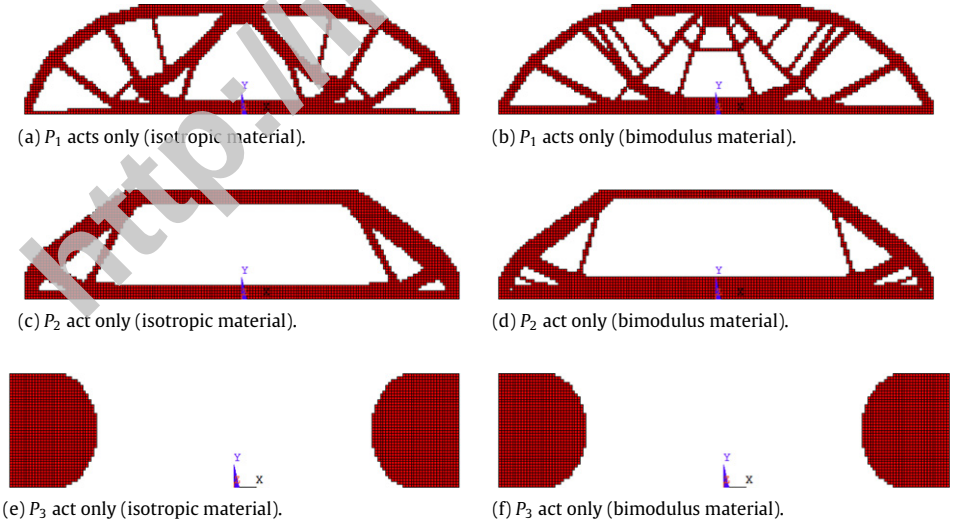

(a) P_1 acts only (isotropic material). (b) P_1 acts only (bimodulus material).

(c) P_2 act only (isotropic material). (d) P_2 act only (bimodulus material).

(e) P_3 act only (isotropic material). (f) P_3 act only (bimodulus material).

Fig. 15. Optimal layouts of structure under different single load cases.

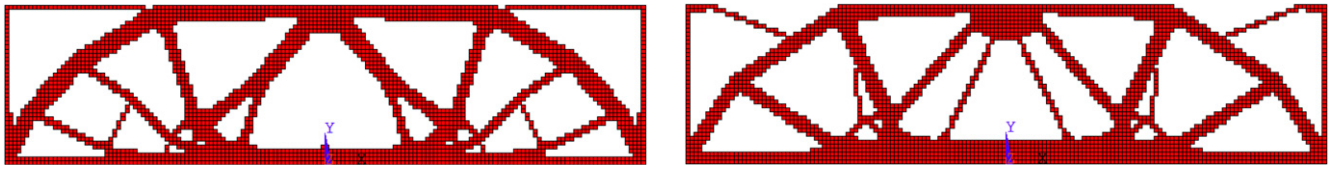

(a) With isotropic material (CPU time: 3935 s). (b) With bimodulus material, $R_{TCE} = 1/5$ (CPU time: 5275 s).

Fig. 16. Topologies of structure with different materials under MLC.

References

[1] Maier G. Limit design in the absence of a given layout: a finite element, zero–one programming problem. In: Gallagher RH, Zienkiewicz OC, editors. Optimum structural design-theory and applications. London: John Wiley & Sons; 1973. p. 223–39.
[2] Atrek E. SHAPE: a program for shape optimization of continuum structures. In: Brebbia CA, Hernández S, editors. Computer aided optimum design of structures: applications. Berlin: Computational Mechanics Publications, Springer-Verlag; 1989. p. 135–44.
[3] Atrek E. SHAPE: a structural shape optimization program. In: Hornlein HREM, Schittkowski K, editors. Software systems for structural optimization. Basel: Birkhäuser Verlag; 1993. p. 229–49.
[4] Rodriguez-Velazquez J, Seireg AA. Optimizing the shapes of structures via a rule-based computer program. Computers in Mechanical Engineering 1985; 4(1):20–8.
[5] Bendsøe MP, Kikuchi N. Generating optimal topologies in structural design using a homogenization method. Computer Methods in Applied Mechanics and Engineering 1988;71:197–224.
[6] Rozvany GIN, Zhou M, Birker T. Generalized shape optimization without homogenization. Structural Optimization 1992;4:250–2.
[7] Rozvany GIN, Kirsch U, Bendsøe MP, Sigmund O. Layout optimization of structures. Applied Mechanics Reviews 1995;48(2):1579–605.
[8] Xie YM, Steven GP. A simple evolutionary procedure for structural optimization. Computers & Structures 1993;49(5):885–96.
[9] Sigmund O. Materials with prescribed constitutive parameters: an inverse homogenization problem. International Journal of Solids and Structures 1994; 31(7):2313–29.
[10] Wang MY, Wang X, Guo D. A level set method for structural topology optimization. Computer Methods in Applied Mechanics and Engineering 2003; 192(1):227–46.
[11] Eschenauer HA, Olhoff N. Topology optimization of continuum structures: a review. Applied Mechanics Review-ASME 2001;54(4):331–90.
[12] Bendsøe MP, Sigmund O. Topology optimization: theory, methods, and applications. Berlin, Heidelberg: Springer; 2003.
[13] Maute K, Frangopol DM. Reliability-based design of MEMS mechanisms by topology optimization. Computers & Structures 2003;81(8–11):813–24.
[14] Luo Z, Tong L, Ma H. Shape and topology optimization for electrothermo mechanical microactuators using level set methods. Journal of Computational Physics 2009;228(9):3173–81.
[15] Kohn RV. Composite materials and structural optimization. In: Proc. workshop on smart/intelligent materials and systems. Honolulu: Technomic Press; 1990.
[16] Kang Z, Tong LY. Integrated optimization of material layout and control voltage for piezoelectric laminated plates. Journal of Intelligent Material Systems and Structures 2008;19(8):889–903.
[17] Paulino GH, Silva ECN, Le CH. Optimal design of periodic functionally graded composites with prescribed properties. Structural and Multidisciplinary Optimization 2009;38(5):469–89.
[18] Luo Z, Luo Q, Tong L, Gao W, Song C. Shape morphing of laminated composite structures with photostrictive actuators via topology optimization methods. Composite Structures 2011;93(2):406–18.
[19] Dühring MB, Jensen JS, Sigmund O. Acoustic design by topology optimization. Journal of Sound and Vibration 2008;317(3–5):557–75.
[20] Andreasen CS, Gersborg AR, Sigmund O. Topology optimization of microfluidic mixers. International Journal for Numerical Methods in Fluids 2009;61(5): 498–513.
[21] Díaz AR, Sigmund O. A topology optimization method for design of negative permeability metamaterials. Structural and Multidisciplinary Optimization 2010;41(4):163–77.
[22] Ambartsumyan SA. Equations of the theory of thermal stresses in double-modulus materials. In: Proceedings of the IUTAM symposium. East Kilbride-Vienna and New York: Springer-Verlag; 1970.
[23] Ambartsumyan SA. On determination of certain mechanical characteristics of materials heteroresistant to tension and compression. The deformation and the rupture of solids subjected to multiaxial stresses. Colloque International. Cannes; 1972.
[24] Medri G. A nonlinear elastic model for isotropic materials with different behavior in tension and compression. Transactions of the ASME 1982;104(1): 26–8.
[25] Desmorat B, Duvaut G. Compliance optimization with nonlinear elastic materials application to constitutive laws dissymmetric in tension–compression. European Journal of Mechanics, A/Solids 2003;22(2):179–92.
[26] Chang CJ, Zheng B, Gea HC. Topology optimization for tension/compression only design. In: Proceedings of the 7th world congress on structural and multidisciplinary optimization; 2007. p. 2488–95.
[27] Liu ST, Qiao HT. Topology optimization of continuum structures with different tensile and compressive properties in bridge layout design. Structural and Multidisciplinary Optimization 2011;43(3):369–80.
[28] Rozvany GIN. A critical review of established methods of structural topology optimization. Structural and Multidisciplinary Optimization 2009;37(3): 217–37.
[29] Guan H, Steven GP, Xie YM. Evolutionary structural optimization incorporating tension and compression materials. Advances in Structural Engineering 1999; 2(4):273–88.
[30] Guan H, Chen YJ, Loo YCH, Xie YM, Steven GP. Bridge topology optimization with stress, displacement and frequency constraints. Computers & Structures 2003;81(3):131–45.
[31] Alfieri L, Bassi D, Biondini F, Malerba PG. Morphologic evolutionary structural optimization. In: Proceedings of the 7th world congress on structural and multidisciplinary optimization. Seoul, Korea; 2007. Paper A0422.
[32] Cai K, Shi J. A heuristic approach to solve stiffness design of continuum structures with tension/compression-only materials. In: Proceedings of the 4th international conference on natural computation. vol. 1; 2008. p. 131–5.
[33] Srithongchai S, Dewhurst P. Comparisons of optimality criteria for minimum-weight dual material structures. International Journal of Mechanical Sciences 2003;45(11):1781–97.
[34] Querin OM, Victoria M, Marti P. Topology optimization of truss-like continua with different material properties in tension and compression. Structural and Multidisciplinary Optimization 2010;42(1):25–32.
[35] Cai K. A simple approach to find optimal topology of a continuum with tension-only or compression-only material. Structural and Multidisciplinary Optimization 2011;43(6):827–35.
[36] Díaz AR, Bendsøe MP. Shape optimization of structures for multiple loading conditions using a homogenization method. Structural Optimization 1992;4: 17–22.
[37] Bendsoe MP, Diaz AR, Taylor EJ. Optimal design of material properties and material distribution for multiple loading condition. International Journal for Numerical Methods in Engineering 1995;38(7):1149–70.
[38] Luo Z, Yang JZ, Chen LP. A hybrid fuzzy-goal programming scheme for multi-objective topology optimization of static and dynamic structures under multiple loading conditions. Structural and Multidisciplinary Optimization 2006;31(1):26–39.
[39] Sui YK, Du JZ, Guo YQ. Topological optimization of frame structures under multiple loading cases. Computational Methods 2006;PTS1&2:1015–22.
[40] Duysinx P. Topology optimization with different stress limit in tension and compression. In: Proceedings of the third world congress of structural and multidisciplinary optimization, WCSMO3; 1999.
[41] Luo YJ. Topology optimization of pressure-dependent material structures based on D–P criterion. Chinese Journal of Theoretical and Applied Mechanics 2011;43(5):878–85.
[42] Bendsøe MP, Sigmund O. Material interpolation schemes in topology optimization. Archive of Applied Mechanics 1999;69(9–10):635–54.
[43] Bendsoe MP. Optimization of structural topology, shape and material. Berlin: Springer; 1995.
[44] Sigmund O. A 99 line topology optimization code written in Matlab. Structural Multidisciplinary Optimization 2001;21(2):120–7.
[45] Sigmund O. Morphology-based black and white filters for topology optimization. Structural and Multidisciplinary Optimization 2007;33(4–5):401–24.
[46] Ansys Inc., Ansys. 2011. http://www.ansys.com.

Kun Cai received his B.S. degree from Lanzhou University in 1999, and his Ph.D. degree from Dalian University of Technology in 2008. Currently he is an associate professor at the College of Water Resources and Architectural Engineering, Northwest A&F University, China. He is a visiting fellow at the Australian National University.

Zhaoliang Gao received his B.S. degree from Northwest A&F University in 1993, and his M.S. degree from Northwest A&F University in 1998, and a Ph.D. degree from Northwest A&F University in 2006. Currently he is an associate professor at the Institute of Soil and Water Conservation, Chinese Academic Science and Ministry of Water Resources, Northwest A&F University, China. Previously, he was an associate Major of Zhongmou County, Henan Province, China.

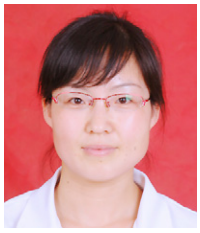

Jiao Shi received her B.S. degree from Lanzhou University in 1999, and her M.S. degree from Northwest A&F University in 2006. Currently, she is a Ph.D. candidate and Lecture at the College of Water Resources and Architectural Engineering, Northwest A&F University, China.